Bioresource Technology 437 (2025) 133009

Contents lists available at ScienceDirect

Bioresource Technology

journal homepage: www.elsevier.com/locate/biortech

Enhancing biochar quality for the steel industry via Hydrothermal Pretreatment-Steam Explosion and pyrolysis

Chay A. Davies-Smith [a,b], Julian Herbert [a,b], Ciarán Martin [a,b,*], Darbaz Khasraw [a,c], David Warren-Walker [d], David Bryant [d], Joe Gallagher [d], Gordon Allison [e], Julian M. Steer [f], Richard Marsh [f], Ahmed Alsawadi [f], Rakesh Bhatia [g]

[a] Tata Steel UK Ltd., Port Talbot, United Kingdom
[b] Swansea University, Swansea, United Kingdom
[c] Advanced Manufacturing & Engineering (AME), Coventry University, Coventry, United Kingdom
[d] Institute of Biological Environmental and Rural Sciences, Aberystwyth University, Aberystwyth, United Kingdom
[e] Department of Life Sciences, Aberystwyth University, Aberystwyth, United Kingdom
[f] Cardiff School of Engineering, Cardiff University, Cardiff, United Kingdom
[g] Department of Agronomy & Plant Breeding, Justus Liebig University Giessen, Giessen, Germany

ARTICLE INFO

Dataset link: DOI: 10.17632/ypbr4mb24w.3

Keywords:
Biorefining
Steel industry
Decarbonisation
Steam explosion
Biochar

ABSTRACT

Biochar has potential applications in steelmaking processes, but faces technical challenges such as low material density, high alkali content, and high reactivity compared to coal. This study explores converting the solid residue, following hydrothermal pretreatment-steam explosion (HTP-SE) of Miscanthus and other biomass feedstocks, into biochar to facilitate the replacement of coal in blast furnace and electric arc furnace operations. It is the first to demonstrate the enhanced combustion characteristics of pretreated fibre and the compatibility of the biochar for use in steelmaking. Biomass from birch, miscanthus, wheat straw, both untreated and pretreated, was evaluated. HTP-SE was conducted at 192 °C and 1.3 MPa, conditions aligned with hemicellulose extraction for application in biobased products. Biochars were produced at temperatures ranging from 300 °C to 550 °C. HTP-SE increased the carbon, hydrogen, and energy content by approximately 10%, 8%, and up to 5 MJ/kg, respectively, while reducing ash quantity by up to 45%. In addition, it reduced the alkali and phosphorus content from the solid fraction into aqueous phase. Gas analysis indicated that HTP-SE enhanced the energy content of pyrolysis syngas. Thermogravimetric studies revealed that pretreated biochars exhibited significantly lower reactivity with carbon dioxide compared to untreated counterparts, approaching the reactivity of coal. This was attributed to increased aromaticity, C=C bonding, cross-linkages enriching lignin and by the removal of hemicellulose through HTP-SE. Overall, the upgraded biochar addresses key limitations of conventional biochar and shows strong potential as a substitute to replace injection coal entirely in both blast and electric arc furnaces.

1. Introduction

Decarbonising the steel industry presents significant economic and technical challenges, and the industry's capacity to invest in these crucial decarbonisation efforts is fundamentally tied to its financial stability. In Europe, steelmakers face financial difficulties arising from stringent environmental policies, emission requirements, and reduced demand for steel. In the UK, steel producers face the additional pressure of some of the world's highest energy prices and high business rates (Hutton et al., 2023). Technically, the challenge is also great. Coal is a key constituent to the blast furnace - basic oxygen furnace (BF-BOF) route, which produces 70.8% of the world's steel, and is also often used alongside natural gas in the operation of an electric arc furnace

* Corresponding author at: Swansea University, Swansea, United Kingdom.
E-mail addresses: Chay.Davies-Smith@tatasteeleurope.com, 2275950@swansea.ac.uk (C.A. Davies-Smith), Julian.Herbert@tatasteeleurope.com (J. Herbert), Ciaran.Martin@tatasteeleurope.com, c.martin@swansea.ac.uk (C. Martin), ae4132@coventry.ac.uk (D. Khasraw), djw17@aber.ac.uk (D. Warren-Walker), dgb@aber.ac.uk (D. Bryant), jbg@aber.ac.uk (J. Gallagher), goa@aber.ac.uk (G. Allison), SteerJ1@cardiff.ac.uk (J.M. Steer), MarshR@cardiff.ac.uk (R. Marsh), alsawadiam@cardiff.ac.uk (A. Alsawadi), rakesh.bhatia@agrar.uni-giessen.de (R. Bhatia).

https://doi.org/10.1016/j.biortech.2025.133009
Received 12 March 2025; Received in revised form 16 July 2025; Accepted 16 July 2025
Available online 7 August 2025

(EAF), with the EAF steelmaking route producing 28.9% of the world's steel (worldsteel, 2022).

Despite economic and technical limitations, the steel industry will need to continue utilising carbon sources in the foreseeable future. To comply with climate change and sustainability legislation, steel producers must find ways to offset GHG emissions. One such avenue could be replacing fossil carbon with sustainably sourced biomass carbon. Lignocellulosic biomass from agroforestry, dedicated biomass crops or agricultural residues, are Earth's most abundant renewable bioresource (Wang et al., 2021). It is chiefly comprised of the polysaccharides, cellulose (40%–60%) and hemicellulose (20%–35%), and the aromatic polymer, lignin (15%–40%), on a dry matter basis (Zoghlami and Paës, 2019). The use of biomass-based carbon in the steel industry is not new. Historically, blast furnaces operated with a charcoal charge; however, this was superseded by coke as the superior mechanical properties of the latter allowed for the construction of larger, more efficient blast furnaces (Feliciano-Bruzual, 2014). In Brazil, some steelmakers still utilise charcoal in the charge of smaller-scale blast furnaces, whilst in the rest of the world, several blast furnace operators have used biochar as a replacement for pulverised/granulated coal injection (PCI/GCI) (Feliciano-Bruzual, 2014; Mathieson et al., 2011). In the European Union, extensive research and trials on using biochar in EAFs have occurred under the GREENEAF and GREENEAF2 projects (Bianco et al., 2013; Cirilli et al., 2018). Several factors have limited the widespread adoption of biomass to replace coal in EAFs in the steel industry: (1) Raw biomass has far lower energy and carbon content than coal; (2) It requires thermal treatment to produce biochar with a higher heating value (3) The purchase price of biochar on the open market is significantly higher, up to $500 for biochar compared to $200 for coal; and (4) High alkali and phosphorus contents in the biochar can lead to technical issues in blast furnace operation, caused by poor slag foaming (Bianco et al., 2013; Cirilli et al., 2018). Hydrothermal carbonisation (180 °C–240 °C, 0.5 to 8 h at 10–25 MPa), producing hydrochar, has received attention for steelmaking in the EAF, and it is an effective slag-foaming agent (Cardarelli and Barbanera, 2023; Wei et al., 2024). However, studies focused on BF operations have concluded that hydrochar is unsuitable for replacing 100% of the injection coal and that blending is recommended (Amado-Fierro et al., 2023; Sarker et al., 2024). Notably, the hydrochar production process has not been commercialised on an industrial scale and degrades labile carbohydrates that could otherwise serve as a value stream to improve process economics. Although dependent on high pressure and steam, hydrothermal pretreatment (HTP-SE) by steam explosion (SE) is described as one of the most efficient and environmentally friendly processes for the pretreatment of lignocellulosic biomass (Shrotri et al., 2017; Ziegler-Devin et al., 2021). First originating in 1927 with the Masonite process, SE has been widely utilised in the paper and pulp industry (Suchsland et al., 1987). In this process, lignocellulosic biomass is heated with high-pressure steam in the temperature range of 150–260 °C (0.47–4.69 MPa) and held at a residence time of several minutes before rapid decompression to atmospheric pressure, hence the term steam explosion (Ahmad and Pant, 2018; Shrotri et al., 2017; Ziegler-Devin et al., 2021). Adjusting these process parameters can achieve over 80% depolymerisation, solubilisation and extraction of the more labile hemicellulose from the insoluble fibre. This results in the formation of xylooligosaccharide syrups and/or monomers such as xylose and arabinose sugar streams, along with thermal degradation products like furan-2-carboxaldehyde (Bhatia et al., 2021; Walker et al., 2018). The hemicellulosic fraction is the least energy-dense portion of the material, with a high heating value (HHV) of around 13.9 MJ/kg, compared to measured values of 16.5 MJ/kg and 20.4 MJ/kg for cellulose and lignin, respectively (Kim et al., 2017). Removing the hemicellulose from the solid fraction produces a more energy-dense solid product, which has seen HTP-SE being utilised more recently in the power industry to make "black" pellets for combustion. Black pellets, therefore, have a higher specific energy content, improved mechanical properties, and are hydrophobic (Strauss and Schmidt, 2018). HTP-SE is an industrially scalable and commercialised process deployed globally to pretreat biomass with technologies from companies such as Valmet, Cambi, and Andritz. The hemicellulose extracted by HTP-SE can be valorised by biorefining routes to higher value products, such as xylo-oligosaccharide prebiotics, xylitol, furfural etc., with estimated market values of 144.5 million by 2033, 1.4 Bn by 2025 and 767 million USD by 2028 respectively (Custom Market Insights, 2024; Future Market Insights Inc, 2023; Markets and Markets, 2023) creating an additional revenue stream (Walker et al., 2018). Therefore, integrated biorefining of lignocellulosic biomass offers multiple advantages: (1) extracting the more labile hemicellulose fraction can enhance the solid fibre's suitability for the steel industry by increasing its higher heating value (HHV); (2) the extracted hemicellulose can boost the process's economics; and (3) reducing both the ash quantity and the alkali content of the material by partitioning into the aqueous phase (Bin and Hongzhang, 2010; Wolbers et al., 2018). This is particularly important to steel industry applications as it may prevent the addition of undesirable elements, such as potassium, into the steelmaking process. This research aims to investigate a novel use for the HTP-SE solid fraction for steel production. It seeks to bridge a knowledge gap in the use of biomass for steelmaking by evaluating the quality of the upgraded pyrolysed solid residue, ensuring its suitability for high-value applications in BF-BOF and EAF processes. A comparison is made between the reactivity, carbon, ash, and energy contents of conventional biochar from birch, miscanthus, and wheat straw with biochar derived from these materials that have undergone HTP-SE. It is hypothesised that HTP-SE could sufficiently upgrade biochar currently of marginal quality for steelmaking to become a viable alternative for existing steelmaking fossil carbon sources (coal, coke, etc.). While multiple biochar production techniques exist, there is a paucity of publications (Li et al., 2024; Yu et al., 2022) describing the use of HTP-SE in combination with pyrolysis to upgrade biomass for higher value applications. As far as we know, this is the first report demonstrating how biomass combustion and quality enhancements via HTP-SE can make multiple feedstocks viable for steel production globally.

2. Materials and methods

2.1. Materials

Miscanthus *x* giganteus *(MxG)* was harvested at Aberystwyth University, UK and air-dried to <15% w/w moisture content; wheat straw was obtained from R J Edwards agricultural suppliers, Aberystwyth, UK; and silver birch was harvested during the remediation of land owned by Tata Steel around the Llanwern steelworks, UK. Feedstocks were milled to <40 mm using an Electra 15 kW BC grinding mill before pretreatment by HTP-SE. These materials were chosen to represent the three biomass sources identified as suitable for utilisation within the steel industry: agricultural byproducts, forestry, and energy crops.

2.2. Methods

2.2.1. Hydrothermal pretreatment

HTP-SE was performed to maximise hemicellulose hydrolysis and extraction from the biomass and a detailed explanation is described in previous work by the authors (Walker et al., 2018). Imbibing and HTP-SE of the biomass and washing of the residual solids were optimised to maximise hemicellulose yield, therefore the residual solids are representative of the byproduct from a hemicellulose extraction process. Briefly, 500 g of biomass was imbibed with a 1:10 solid:liquid ratio with 1% w/v phosphoric acid at 50 °C for 16 h, drained and loaded into a 30 L Cambi steam explosion unit. The HTP-SE conditions for maximum hemicellulose removal and solubilisation were 1.3 MPa for 6 min; subsequently, the chamber pressure was increased to 1.6

MPa before undergoing instantaneous decompression to atmospheric pressure, and the residual solids were ejected into a collection vessel.

A combined severity factor of 1.6, R_0, described by the conditions above, was calculated using the adapted Overend & Chornet, 1987 method, shown in Eq. (1) (Overend and Chornet, 1987; Abatzoglou et al., 1992; Pedersen and Meyer, 2010). Where t is the residence time in minutes, which was 6 min; T is the temperature of pretreatment, which was 192 °C; 14.75 is the arbitrary constant ω, which is the activation energy from first-order kinetics; and 100 °C is the reference temperature, and pH is the pH of the material entering the SE vessel, 1.9 (±0.1).

$$(Log R_0) = Log(R_0 \cdot [H^+]) = Log R_0 - pH = \left[R_0 = t \cdot e \cdot \frac{T-100}{14.75}\right] - pH \quad (1)$$

Following HTP-SE, the material was cooled to <50 °C and water-soluble carbohydrates were recovered from the solids through manual counter-current washing using a Vincent Corp CP4 screw-press and the dewatered fibre was oven-dried at 80 °C. The dried fibre was adjusted to 16% moisture content before pelleting and rapeseed oil (5% w/w) was added as a binder. The material was homogenised by vigorous mixing and pelleting using a Simon Barron Hyflo pellet mill. The pellet mill was prewarmed with a mixture of grass fibre and grass fibre pellets for 30 min, which ensured that the die was at a sufficient temperature to melt the lignin and create a stable pellet. The 300 mm internal diameter pellet die, contained 198, 6 mm diameter pellet holes and was operated at 192 rpm with a feed rate of 1.9 kg/minute.

2.2.2. Production of biochar

Biochar was prepared by the heat treatment of biomass in the absence of air. While it is acknowledged that there is a defined difference between torrefaction and pyrolysis based upon the temperature of the thermal treatment, for the ease of communication, only the term pyrolysis is used throughout this work.

To prepare the biochar samples used in the majority of this study, preheated cylindrical crucibles with well-fitting lids, as used in the determination of volatile matter, were filled with around 10 g of biomass and placed in a muffle furnace at a range of temperatures and for a range of times. Between 4 and 8 crucibles were used at any one time. These cylindrical crucibles allowed for a more consistent heat distribution than larger crucibles, producing more repeatable results.

The biochars used in the ultimate analysis were pyrolysed to completion. Specifically, the time they spent in the furnace was determined based on the required pyrolysis time calculated in the thermogravimetric analysis experiments, with additional time added to allow for the poorer heat flow in the muffle furnace. The 350 °C chars were heated for 40 min, whilst the 450 °C and 550 °C chars were heated for 20 min.

2.2.3. Proximate analysis

Proximate analysis details the amount of moisture, ash, volatile matter and fixed carbon in a solid fuel. All work was conducted on a dry basis. Hence samples were dried prior to proximate analysis and laboratory tests, so moisture content was disregarded. Fixed carbon was calculated by difference. Ash and volatile matter was determined using BS EN ISO 18122:2022 and BS EN ISO 18123:2023, respectively. Drying was undertaken before testing by heating the samples in an oven at 105 °C for an hour, before being cooled in a desiccator.

$$C_{fix} = 100 - (A + V) \quad (2)$$

Fixed carbon (C_{fix}) was calculated via Eq. (2), as described in BS ISO 17246:2010. The ash (A) was measured in accordance with BS EN ISO 18122:2022. Ash is the remaining residue after the biomass has been incinerated in air and is derived from inorganic complexes present in the original sample and associated mineral matter. Using BS EN ISO 18122:2022, biomass/biochar samples were heated to 250 °C and held for an hour before being heated to 550 °C and held for a minimum of 2 h to establish the ash mass. The volatile matter (V) was measured using the method described in BS EN ISO 18123:2023. The volatile matter was determined as the mass portion lost when the sample was heated in the absence of air at 900 °C for 7 min.

2.2.4. Determination of structural carbohydrates and lignin

Using NREL laboratory analytical procedures, carbohydrate content was quantified in both the fibre and hydrolysates fractions (Sluiter et al., 2008, 2012). HTP-SE hydrolysate was cooled to room temperature and stored until required at −20 °C. 300 mg of freeze-dried biomass material was added to 3 mL 72% H_2SO_4 and mixed at 30 °C for 60 min, diluted to 4% v/v H_2SO_4 by the addition of 84 mL deionised water, autoclaved at 121 °C for 60 min, cooled to room temperature and neutralised to pH 6 with $CaCO_3$. To quantify the monomer to polymer ratio, liquid hydrolysate from HTP-SE was acid hydrolysed by adding 34.8 μL of 72% H_2SO_4 to 1 mL of hydrolysate, followed by autoclaving and neutralisation as described above.

2.2.5. Thermogravimetric analysis - pyrolysis of biomass

A Mettler-Toledo TGA/DSC 3+ was used to conduct thermogravimetric analyses on the biomass samples. The biomass samples were dried, pyrolysed, devolatilised, and gasified during the analysis. This determined the required pyrolysis time, yield, biochar volatile matter, and gasification reactivity. The procedure used to generate this data is described below:

Between 20–30 mg of ground sample was heated to 105 °C at a rate of 50 °C/min in a 50 ml/min flow of N_2 and held for 10 min to remove any reabsorbed moisture, then heated to the test temperature at a rate of 50 °C/min. At test temperatures of 300–400 °C, samples were held for 2 h, whereas at 450–550 °C, samples were held for 1 h. The sample was then heated to 900 °C at a rate of 50 °C/min and held for 7 min to remove the volatiles, followed by gasification for 2 h at 900 °C in a 100 ml/min flow of CO_2. CO_2 was used to facilitate char gasification via the reverse Boudouard reaction, as shown in Eq. (3).

$$C + CO_2 \rightarrow 2CO \quad (3)$$

All analyses were calculated on a dry basis. Therefore, the initial dry mass of the sample (m_d) and initial time value (t_d) were taken as the first values after the drying portion of the programme was performed. The mass loss during pyrolysis was defined as the difference between m_d and the mass at the end of the pyrolysis portion of the programme (m_p). The ash of the material was considered in the calculation to analyse the effect of the HTP-SE on the lignocellulosic portion of the material. The ash-free biochar yield (Y_{af}) of the pyrolysis was calculated using Eq. (4).

$$Y_{af} = \left(\frac{m_p}{m_d} \times 100\right) - A \quad (4)$$

As the mass loss during pyrolysis was an exponential decay, it was necessary to define a point at which the pyrolysis was deemed complete and the endpoint (t_{m95}) was defined as the time at which 95% of the mass loss was achieved. This was used to calculate the required pyrolysis time (t_p) in minutes in Eq. (5).

$$t_p = \frac{t_{m95} - t_d}{60} \quad (5)$$

The volatile matter (V_{TGA}) of the remaining biochar was calculated using the difference in mass at the end of the devolatilisation step of the programme (m_{dv}) and m_p in Eq. (6).

$$V_{TGA} = \frac{m_p - m_{dv}}{m_p} \times 100 \quad (6)$$

The remaining biochar gasification reactivity was then determined using the mass loss in the final gasification step of the programme. This was done using Eq. (7) below.

$$x = \frac{m_{dv} - m}{m_{dv} - m_g} \quad (7)$$

Where x is the char conversion, m is the instantaneous mass, and m_g is the mass at the end of the gasification step.

Samples were run in duplicate and average values were calculated. To measure the error in this method, a set of analyses was conducted with 7 repeats, and the percentage error was calculated at each test temperature using the standard deviations. This was undertaken with the steam-exploded miscanthus sample.

2.2.6. Thermogravimetric analysis - kinetic modelling

The Mettler-Toledo TGA/DSC 3+ was used to perform the gasification experiments for the kinetic modelling. A detailed assessment of the TGA and kinetic modelling method has been written in another publication (Alsawadi et al., 2025).

In this work, isothermal tests were performed in duplicate in the TGA at 850 °C, 900 °C, 950 °C and 1000 °C on the six 550 °C biochars. Prior to testing in the TGA, the chars were dried and ground to 75 μm to control for the effect of particle size on reaction rate. Samples were heated to 900 °C at a rate of 20 °C/min in 100 ml/min of N_2, and then held for 7 min to devolatilise. They were then raised to selected test temperature and held in CO_2 at the same flow rate, until no further mass loss occurred. In practice, this ranged from as long as 2000 min for HTP-SE materials at 850 °C to 40 min for non-HTP-SE materials at 1000 °C.

Kinetic modelling of CO_2 gasification was performed to determine the impact of HTP-SE on biochar reactivity. Activation energy was of particular interest as this indicates fundamental differences in the reactivity of the materials and the suitability of HTP-SE solid residue biochar for use in steelmaking. Three models were used: volumetric, grain, and random pore. This was necessary to verify whether activation energy was similar across different models. The volumetric model assumes that gas-solid reactions occur equally at all char particles' internal and external active sites. The grain model assumes that particles are spherical and consumed from the outside surface so that the particle shrinks until only ash remains. Random pore model takes account of overlapping of pores and that as the reaction proceeds, these can merge into one as char is consumed during gasification (Wang et al., 2015, 2016).

2.2.7. Ultimate analysis

Ultimate analysis was conducted on a ThermoFisher Scientific FlashSmart Elemental Analyzer. Ultimate analysis gives the amounts of carbon, hydrogen, nitrogen and sulphur in a fuel sample with oxygen being calculated by difference. 2–4 mg of sample was used per measurement and analysis was conducted in duplicate. The instrument was calibrated using a 2,5-Bis(5-tert-butyl-2-benzo-oxazol-2-yl) thiophene (BBOT) standard containing 6.48% nitrogen, 72.51% carbon, 6.08% hydrogen, and 7.42% sulphur.

The ultimate analysis was used to calculate the high heating value of the fuel using Eq. (8) (Qian et al., 2020).

$$HHV = 32.9\left(\frac{C\%}{100}\right)+162.7\left(\frac{H\%}{100}\right)-16.2\left(\frac{O\%}{100}\right)-954.4\left(\frac{S\%}{100}\right)+1.408 \quad (8)$$

The ultimate analysis was also used to calculate the fuel's coke replacement ratio (RR), a commonly used value in the steel industry. This was calculated using Eq. (9) (Geerdes et al., 2020).

$$RR = 0.998\left(\frac{C\%}{100}\right)+2.217\left(\frac{H\%}{100}\right)-0.077\left(\frac{O\%}{100}\right)-0.067\left(\frac{N\%}{100}\right) -0.073\left(Q_{crack}\cdot\frac{100-moist}{100}\right)-1.1\left(\frac{moist}{100}\right) \quad (9)$$

Where the cracking heat, or heat of decomposition (Q_{crack}), was calculated using Eq. (10), using the volatile matter (V) calculated in Section 2.2.3 (Geerdes et al., 2020). Moisture content, $moist$, was 0 as all work was conducted on a dry basis.

$$Q_{crack} = 0.0007\cdot V^2 + 0.0126\cdot V - 0.3687 \quad (10)$$

2.2.8. Regression analysis

Polynomial regression was used to quantify the effect of the HTP-SE process in cases where multiple data points were available across a temperature range. For each biomass–HTP-SE pair and each variable, a cubic polynomial regression model was fitted using ordinary least squares:

$$Y = \beta_0 + \beta_1 T + \beta_2 T^2 + \beta_3 T^3 + \beta_4 \cdot Sample_{HTP-SE} + \varepsilon \quad (11)$$

Where: Y is the response variable; T is the pyrolysis temperature in °C; $Sample_{HTP-SE}$ is a binary indicator variable for sample type (0 = untreated, 1 = HTP-SE); $\beta_0, \beta_1, \beta_2, \beta_3, \beta_4$ are the regression coefficients; ε is the error term. For each model, the following metrics were extracted:

- Adjusted R^2: Indicates the proportion of variance explained, adjusted for model complexity.
- Sample Effect (β_4) and p-value: Quantifies the average difference in the response variable between HTP-SE and untreated samples, after adjusting for temperature. A p-value < 0.05 was considered statistically significant.

2.2.9. Analysis of biomass ash

The biomass ashes were analysed at Tata Steel UK's Port Talbot Basic Oxygen Steelmaking (BOS) plant laboratory. The ash samples were generated by heating 100 g of sample, spread thinly across multiple large crucibles, to 250 °C and holding for an hour, before heating the sample to 550 °C and holding the temperature for a minimum of 2 h, ensuring complete combustion of the sample, whereupon no further mass loss was observed.

The ash provided to the laboratory was analysed using X-ray fluorescence (XRF) and inductively coupled plasma optical emission spectroscopy (ICP-OES). The XRF analysis was conducted on an Axios XRF Spectrometer. The ash was mixed with lithium tetraborate:metaborate flux and heated in platinum dishes in a TheOx bead maker furnace until molten. The molten sample was poured into heated platinum moulds that were then cooled to room temperature. The solid beads were then analysed using XRF. The XRF analysis provided the ashes' Si, Al, Ca, Mg, P, Ti, and Fe contents. 0.25 g of ash was digested in 40% concentration HF and 37% concentration HCl and diluted with deionised water to 250 ml prior to use in the analyser. The ICP-OES analysis provided the ashes' Na, K, Zn, and Cu contents.

$$B3 = \frac{CaO + MgO}{SiO_2 + Al_2O_3} \quad (12)$$

Eq. (12) calculates ash B3 basicity using relative ash oxide proportions (Babich et al., 2008).

2.2.10. Analysis of pyrolysis syngas

Gas analysis experiments were performed using a Carbolite Gero high-temperature vertical tube furnace (VTF) with a recrystallised alumina tube VTF-1700/50 (internal diameter 88 mm ×length 1000 mm). The furnace was coupled with a Hiden HPR 20 Quadrupole Mass Spectrometer (QMS) to monitor gaseous products evolving from the samples during heat treatment. The combination of VTF-QMS allowed the biomass samples to be rapidly heated to a pre-set temperature of 550 °C with the off-gas being continuously analysed. Before the experiment started, a sample of approximately 500 mg was placed inside an alumina crucible (27 mm diameter and 31 mm height). This crucible plus sample was suspended from a molybdenum wire and held at the top in a cool region inside the alumina tube. The furnace was heated to a target temperature of 550 °C at a heating rate of 10 °C/min. A carrier gas (Ar, 99.999% purity) at 2 L/min was purged through the furnace from the bottom to create an oxygen-free atmosphere. When the furnace reached the experimental temperature and approximately 99.9% Ar atmosphere, the crucible containing the sample was lowered into the centre of the isothermal region in the furnace, where the pyrolysis took place. The furnace was kept at the pre-set temperature for 30 min while the furnace exhaust was connected to the QMS through a heated capillary (150 °C) to monitor gaseous products evolving from the samples while ensuring no condensation occurred before the ionisation chamber. The QMS was set to measure readings of the following gaseous products: N_2, O_2, CO, CO_2, Ar, H_2O, H_2, CH_4 and C_2H_6.

2.2.11. Scanning electron microscopy

Backscattered electron (BSE) images and energy dispersive X-ray spectroscopy (EDS) analyses were acquired using a Zeiss Sigma 300 variable pressure field emission gun scanning electron microscope (SEM) located in the School of Earth and Environmental Sciences, Cardiff University. The SEM was equipped with a retractable four quadrant solid-state backscattered electron detector and dual Oxford Instruments UltimMax 65 mm^2 EDS detectors. Images and spectra were acquired using Oxford Instruments AZtec software version 6.1. The work was conducted in low vacuum mode, with a chamber pressure of 40 Pa sufficient to neutralise charge build up on the uncoated samples. A beam energy of 15 kV was used with a 60 μm diameter final aperture and a working distance of 8.5 mm. BSE images were acquired using a dwell time of 35 μs while EDS spectra were acquired with a livetime of 15 s per spectrum. The semi-quantitative EDS spectra were background and overlapping peaks corrected, calibrated using factory standards, and are reported normalised to 100%.

2.2.12. Fourier transform infrared spectroscopy

Spectra from the six samples of dried ground 550 °C char were collected in duplicate from 600 to 4000 cm^{-1} using a Nicolet iS50 spectrophotometer using an inbuilt diamond attenuated total reflection (ATR) accessory. Background absorbance from the empty crystal was collected prior to measurement of absorbance spectra. The instrument was operated using proprietary software. Spectra were processed by multiplicative scatter correction to normalise the spectra and correct for base-line deviation. Spectra for each sample were mean-averaged. The difference between the HTP-SE and non-HTP-SE materials was plotted on a mean-adjusted chart to enable the effects of steam explosion to be more clearly visualised.

2.2.13. Blast furnace heat and mass balance (HMB) model

The effect of replacing 100% of the injection coal with regular and HTP-SE biochar was undertaken using a proprietary mathematical blast furnace model that balances the input and output heat and mass in a blast furnace system. The model represents steady-state conditions. Variables including temperatures, mass and heat flow rates, material compositions, ash analyses, hot metal analysis, slag analysis, and gas composition are all taken into account. The inputs and outputs are linked via equations and the model calculates these simultaneously. Variables can be fixed as constants or left free to be calculated. Choosing which to fix and which to calculate enables a user to investigate the effect of specific chosen variables on the blast furnace. In this work, the output variables of interest were the coke rate which indicates the effectiveness of each biochar when compared to coal, and flame temperature which indicates furnace thermal stability.

Injecting coal or biochar into the blast furnace reduces the amount of coke required to operate the blast furnace.

$$\Delta \mathrm{CO}_2 = \frac{44}{12} \times \frac{\Delta Coke}{Y_{Coking}} \times \mathrm{C}_{Coke} \tag{13}$$

Eq. (13) calculates the CO_2 reduction (ΔCO_2) due to the reduction in coke, where 44/12 was the molecular weight of CO_2 divided by the molecular weight of carbon. The ΔCO_2 was calculated as per the HMB model. Dry coke to dry coking coal yield (Y_{Coking}) and coking coal carbon content (C_{Coke}) were 79.3% and 85.8%, respectively, as per historical Port Talbot data. For the biochar injection scenarios, it was assumed that these were carbon neutral based upon sustainable sourcing of biomass and carbon neutral biochar production methods, e.g. utilising waste heat or green energy. The concept of carbon-neutral emissions from biomass combustion is based upon the replanting of any consumed biomass material, thereby reclaiming carbon from the atmosphere during the plant's growth. The topic is discussed in detail in publications such as the UK Government's Biomass Strategy (Department for Energy Security & Net Zero, 2023).

3. Results and discussion

3.1. The effect of HTP-SE on biomass composition

Supplementary Material Table S1 shows the proximate and ultimate analyses of the biomass materials whilst Table S2 (see Supplementary Material) shows the lignocellulosic composition of the biomass materials. Considering the proximate analysis, steam explosion and washing reduced the ash of each biomass feedstock, with respective reductions in ash of 45.1%, 37.2% and 2.7% for birch, Miscanthus, and straw. The reduction in ash prior to pyrolysis is favourable for producing high-quality biochar for application within the steel industry. During biochar reduction, volatile organics are removed whilst inorganics are mostly retained, causing the mineral matter to concentrate within the biochar, resulting in increasing ash with increasing pyrolysis temperature and/or residence time. During blast furnace fuel injection, the fuel's ash consumes high-temperature heat from the raceway to heat and melt it, which would otherwise be utilised to melt the charge (Geerdes et al., 2020). This increases the fuel rate: for example, a 1% increase in ash would result in an increased coke rate requirement of up to 5 kg/t_{HM} (kg per tonne of hot metal produced), dependent on the injection rate (Babich et al., 2008). Over sustained periods of operation, small increases to the coke rate can incur costs of millions of dollars, as such, ash removal from biomass feedstock by HTP-SE prior to biochar production indicates the techno-economic utility of their combined use for steel production. The birch biomass showed an apparent increase in fixed carbon and reduced volatile matter. At the same time, miscanthus and straw exhibited a decrease in fixed carbon and an increase in volatile matter.

Considering the ultimate analysis, the carbon and hydrogen contents of the HTP-SE biomass were increased while the oxygen content was reduced. This was attributed mainly to the removal of hemicellulose, as shown in Table S2 (see Supplementary Material), and through the removal of a proportion of the mineral matter, as shown in the reduction of ash in Table S1. Sulphur was so low as to be beyond the limit of detection of the analytical apparatus used in this study. Low sulphur is a distinct advantage over coal when considering its application within the steel industry. Sulphur in the steel product causes "hot shortness"; which is increased brittleness in a heated state. The removal of sulphur from the hot metal (liquid iron produced in the blast furnace) decreases process efficiency and increases fuel rates, emissions, and costs (Davies-Smith et al., 2022). The increase in carbon and hydrogen content, as well as the decrease in oxygen, is beneficial for both the HHV and RR of the materials. This is discussed further in Section 3.2.2.

Table S2 (see supplementary materiaL) shows the structural carbohydrates and lignin for the different biomasses and their HTP-SE counterparts. Cellulose contains glucose molecules, while hemicellulose contains, depending on feedstock sources, pentose monomers (xylose and arabinose) and hexose monomers (mannose, galactose, and lesser quantities of glucose) (Mishra et al., 2022). Table S2 (see supplementary material) shows that HTP-SE leads to a significant removal of xylose which was the principal sugar in hemicellulose; there was also a commensurate drop in the other hemicellulose sugars. As a result of removing hemicellulose, the sample becomes more concentrated in cellulose (glucose molecules) and lignin. Birch and miscanthus demonstrate the greatest enrichment in lignin, while there did not appear to be an enrichment in straw lignin. While contrary to those for birch and miscanthus, these data are in agreement with previous research, which demonstrates that lower HTP-SE temperatures can lead to a reduction in straw lignin concentration compared to untreated straw (Cui et al., 2012). However, the mechanism behind the decreased lignin concentration in straw remains unclear. It is clear that straw shows a significant decrease in xylose and an increase in glucose, which is expected. The rise in lignin is beneficial to the steelmaking industry as this is where stable aromatic carbon, C=C bonding and extensive

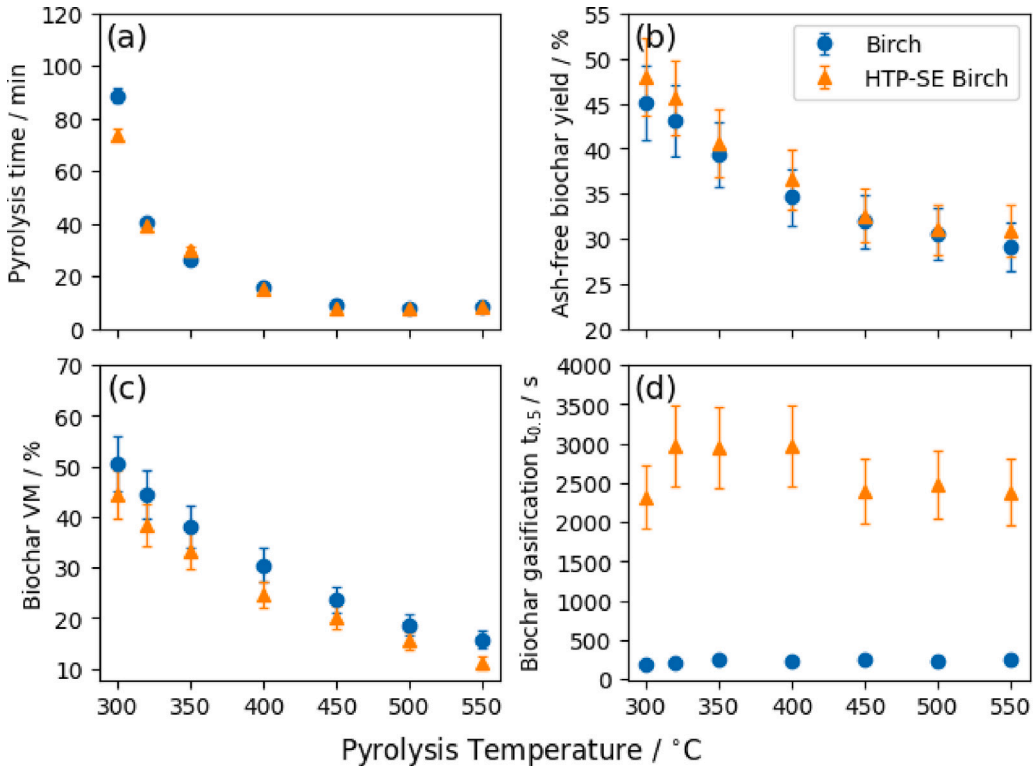

Fig. 1. The effect of HTP-SE on (a) required pyrolysis time, (b) ash-free biochar yield, (c) char volatile matter, (d) char gasification reactivity of birch.

cross-linkages are found, hence, lignin has a higher thermal stability than cellulose and hemicullose (Shen and Gu, 2009; Zhao et al., 2014). It is expected that HTP-SE is assisting in the biochar generation process by a combination of removal of more labile components; concentration of more thermally stable components; removal of catalytic mineral matter elements; and some structural reordering under the hydrothermal conditions, thus helping to create a biochar that is more energy-dense and less reactive than conventional pyrochar. This is attractive for steelmaking where coal is currently used. The increased lignin concentration would theoretically increase the biochar yield when compared to using non-HTP-SE biomass as a pyrolysis feedstock.

3.2. The effect of HTP-SE on biochar production

Raw, untreated biomass is unsuitable for use in current methods of steelmaking. Its properties are too dissimilar from coal and incompatible with established processes. Raw biomass has a lower energy density and contains less carbon than coal. In the blast furnace, one unit of biomass will not replace one unit of coal, which itself is used as a replacement for coke. Injection of raw biomass will therefore require an increase in coke usage, possibly increasing overall costs and fossil fuel use. In the EAF, high reactivity, low density, and poor slag wettability prevent the utilisation of raw biomass (Bianco et al., 2013; Cirilli et al., 2018). Therefore, it is necessary to convert and upgrade biomass to biochar in a heat treatment process to facilitate its use within the steel industry. How the HTP-SE of biomass affects the production of biochar over a range of temperatures has been explored herein. 300 °C was selected as the minimum temperature as this is similar to some of the torrefaction technologies available on the market, whilst 550 °C was selected as the maximum temperature as this is comparable with some of the marketed biochar/biocoal pyrolysis technologies.

3.2.1. The effect of HTP-SE on biochar pyrolysis time, yield, volatile matter, and gasification reactivity

Fig. 1 shows the effect of HTP-SE on the required pyrolysis time, ash-free biochar yield, char volatile matter, and char gasification reactivity of birch samples over a temperature range. Pyrolysis time is of interest because it dictates the pyrolysis process parameters, such as temperature, sizing, and throughput, that can be supported when relying on steelworks waste heat for a chosen amount of biochar to be generated. Regression analysis of the data in this section is shown in Table S3 and referred to for the purposes of quantifying the sample effect and statistical significance (p-value) as a result of HTP-SE. The required pyrolysis time for birch was largely unaffected by HTP-SE; Sample Effect = −0.0302, p-value = 0.6823. The ash-free biochar yield was slightly increased following HTP-SE and this was statistically significant; Sample Effect = 0.8429, p-value = 0.0232. The volatile matter of the produced biochar was reduced across all test temperatures; Sample Effect = −4.8571, p-value < 0.001. The lower volatile matter is beneficial for improving the RR of the biochar, which is discussed further in Section 3.2.2. The greatest difference was seen in the biochar gasification reactivity. The results of this experiment are expressed in the gasification time $t_{0.5}$, which is the time taken to achieve 50% char conversion. The lower the $t_{0.5}$ number, the more reactive the char (Sexton et al., 2018; Davies-Smith et al., 2022). 900 °C was selected as the experimental temperature for the gasification step as this temperature had previously been used in the study of blast furnace injection coals as it is a temperature that can be found in the blast furnace above the cohesive zone where unburnt char may accumulate and interact with gaseous CO_2 (Sexton et al., 2018; Steer et al., 2018). This allowed for comparison of the biochar char gasification reactivity with historical coal data. The HTP-SE birch was substantially less reactive than untreated birch; Sample Effect = 2.4417, p-value < 0.001, taking around 2000 s longer to gasify half of the material at most test temperatures, which is comparable with more reactive coals (Sexton et al., 2018; Steer et al., 2018). This could help alleviate some of the issues uncovered in using biochar as a slag foaming agent in the GREENEAF projects (Cirilli et al., 2018; Bianco et al., 2013).

Fig. 2 shows the effect of HTP-SE on the required pyrolysis time, ash-free biochar yield, char volatile matter, and char gasification reactivity of miscanthus samples over the range of temperatures studied. HTP-SE led to an apparent increase in the required pyrolysis time;

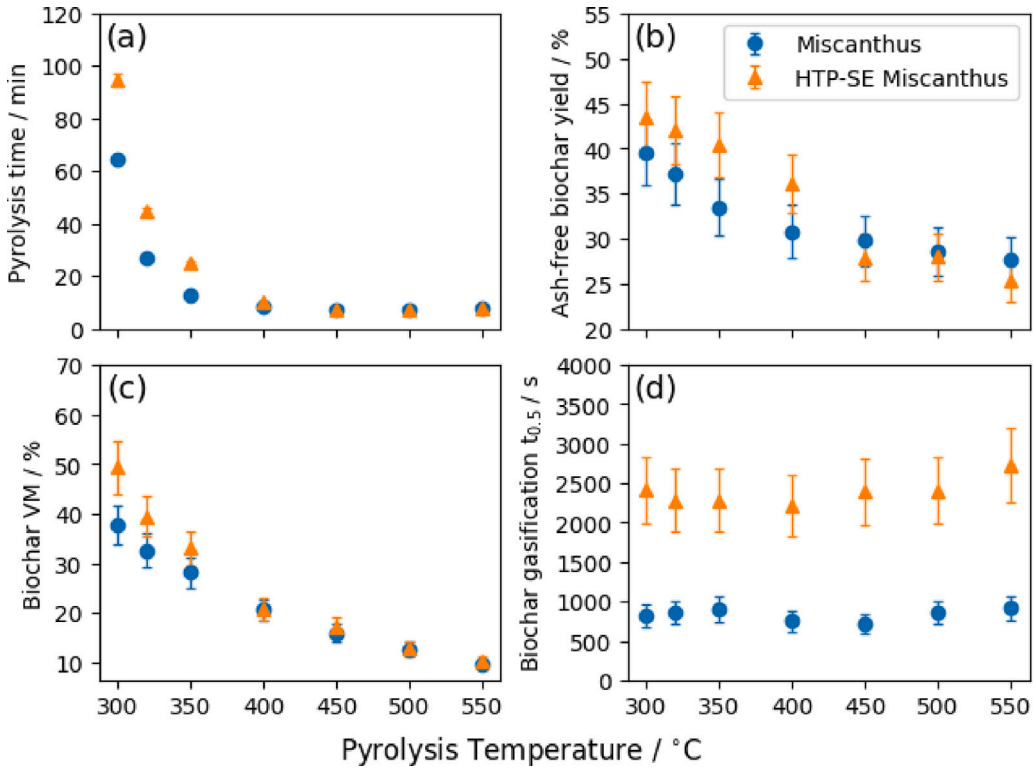

Fig. 2. The effect of HTP-SE on (a) required pyrolysis time, (b) ash-free biochar yield, (c) char volatile matter, (d) char gasification reactivity of miscanthus.

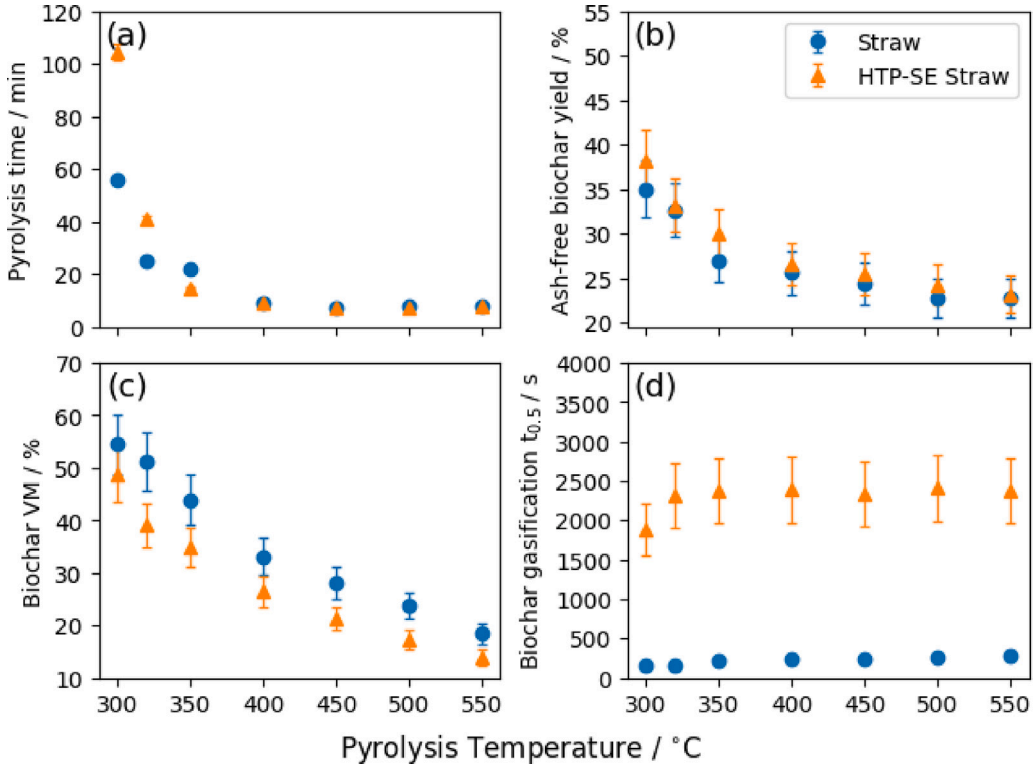

Fig. 3. The effect of HTP-SE on (a) required pyrolysis time, (b) ash-free biochar yield, (c) char volatile matter, (d) char gasification reactivity of straw.

Sample Effect = 0.2492, p-value = 0.0181, notably at the lower temperatures less than 400 °C. The ash-free biochar yield was also higher at lower temperatures; however, the 450 °C, 500 °C, and 550 °C HTP-SE samples demonstrated comparable yields to the untreated samples. An overall positive sample effect but a non-statistically significant p-value of 0.2362 accompanies this data. The difference in yield with temperature may have been caused by the large increase in cellulose and lignin content in the HTP-SE sample, as shown in Section 3.1. This

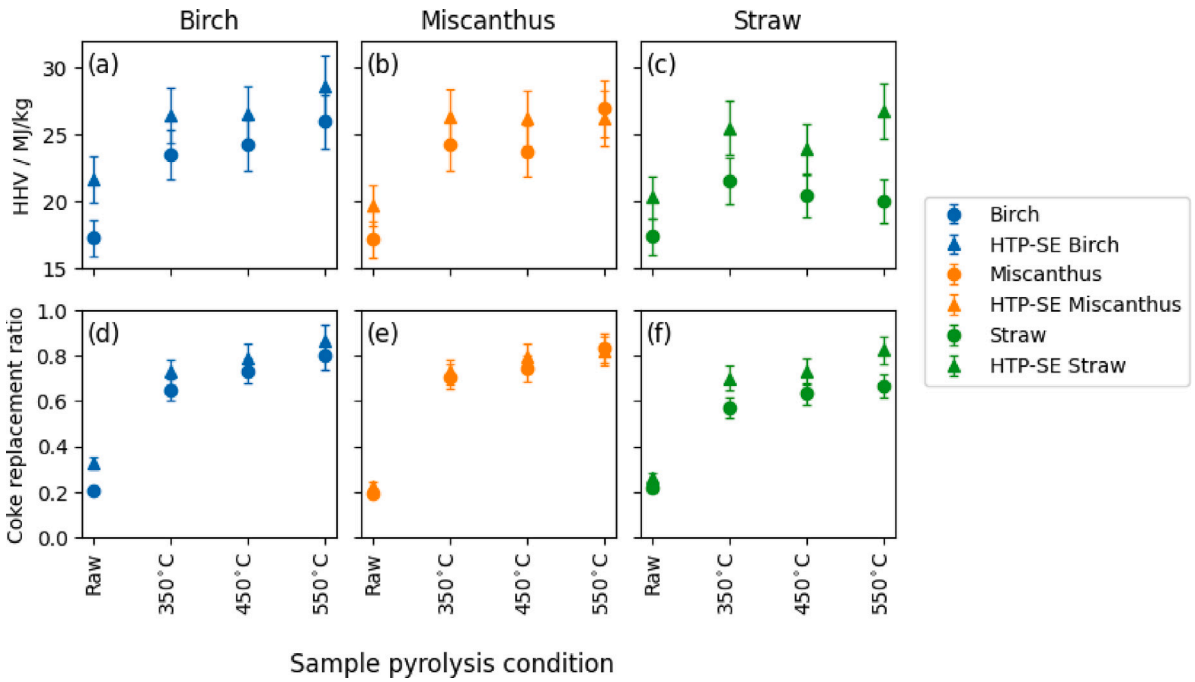

Fig. 4. HHVs (a-c) and Coke Replacement Ratios (d-f) of untreated and HTP-SE biomass and produced biochars.

would show the greatest effect at lower temperatures where cellulose and lignin are less readily thermally decomposed. HTP-SE samples had higher volatile matter contents less than 400 °C but were comparable to untreated samples at higher temperatures; Sample Effect = 3.6286, p-value = 0.0300. HTP-SE clearly decreased the biochar gasification reactivity; Sample Effect = 1.0561, p-value < 0.001.

Fig. 3 shows the effect of HTP-SE on the required pyrolysis time, ash-free biochar yield, char volatile matter, and char gasification reactivity of straw samples over the range of temperatures studied. Like the miscanthus, HTP-SE increased the required pyrolysis time of straw samples at lower temperatures (<350 °C). However, the overall trend was not statistically significant; Sample Effect = 0.0996, p-value = 0.4080. As with the birch samples in Fig. 1, ash-free biochar yield was largely unaffected by HTP-SE; Sample Effect = 0.7571, p-value = 0.1219, whilst HTP-SE reduced biochar volatile matter content across all test temperatures; Sample Effect = −7.3857, p-value < 0.001. HTP-SE significantly reduced the gasification reactivity of the straw biochar; Sample Effect = 2.3689, p-value < 0.001.

All biomass materials showed changes to biochar production when pretreated by steam explosion and washing. The decrease in biochar volatile matter content in the birch and straw samples would result in more favourable coke replacement ratios, whilst the reduced reactivity of all of the pretreated biochars could have beneficial effects when applied in the steel industry. As previously mentioned, biochar's high reactivity was a problem encountered in the GREENEAF projects during the injection of biochar in an EAF, whilst accumulation of highly reactive biochar could lead to instances of localised cooling and an increased coke rate during blast furnace application (Cirilli et al., 2018; Steer et al., 2018). The ideal biochar production conditions will be determined by the application and site specific requirements, such as the availability of waste heat or tuyere injection capacity.

3.2.2. *The effect of HTP-SE on biochar HHV and RR*

Biochar's energy content and coke replacement ratio are key factors in their potential use in the steel industry. Fig. 4a-c shows the calculated HHVs of both the untreated and HTP-SE biomass and biochars produced at 350 °C, 450 °C, and 550 °C. Accompanying regression analysis data for HHV and RR can be found in Table S4. It is typical for HHV to vary by around 2 MJ/kg and for RR to vary by around 10 percent for typical injection coals (Geerdes et al., 2020), so the differences observed between most of the untreated and HTP-SE materials in Fig. 4 are greater than those observed between injection coals in the steel industry. Comparing the HHVs of the untreated and HTP-SE biomass and biochars, it is clear that HTP-SE increased the HHV; however, the miscanthus p-value suggested that this was not statistically significant (p-value = 0.1314). This would be because of the removal of mineral matter and hemicellulose, resulting in the more energy-dense components, cellulose and lignin, becoming concentrated in the biomass, as shown in Section 3.1. The greatest increase in energy density can be seen between the untreated and HTP-SE straw samples; Sample Effect = 4.2624, p-value = 0.0157. This is likely explained by the removal of the greatest quantity of low energy density hemicellulose during pretreatment of the straw, as demonstrated in Section 3.1. HTP-SE birch produced the samples with the greatest energy density. The HTP-SE birch had the lowest ash and oxygen content of the studied materials, thereby giving it the greatest combustible material concentration of all the studied materials.

As the temperature of biochar production increased, there was a slight increase in HHV for the majority of the materials. This is caused by the reduction in oxygen content and the increase in carbon content; however, this will be countered by an accumulation of ash-forming mineral matter, which will appear as oxygen within the ultimate analysis used to calculate HHV (due to calculation by difference). This explains why the untreated straw biochars, which produce the most ash, do not increase in energy density when the pyrolysis temperature is increased. The increase in energy density is beneficial as many systems are limited in the physical volume they can convey. This helps to facilitate the replacement of coal with biomass without the need for additional investment.

The RRs of the untreated and HTP-SE biochars are shown in Fig. 4d-f. RR is highly dependent on the material's carbon content; as such, the highest RRs occur in the samples with the highest degree of carbonisation, which occur at the highest temperatures. HTP-SE increased the RR of the tested feedstock; however, the miscanthus p-value suggested that this was not statistically significant (p-value = 0.1952). As is the case for the HHVs, straw had the greatest increase in RR as a result of HTP-SE; Sample Effect = 0.1076, p-value = 0.0209, whilst HTP-SE

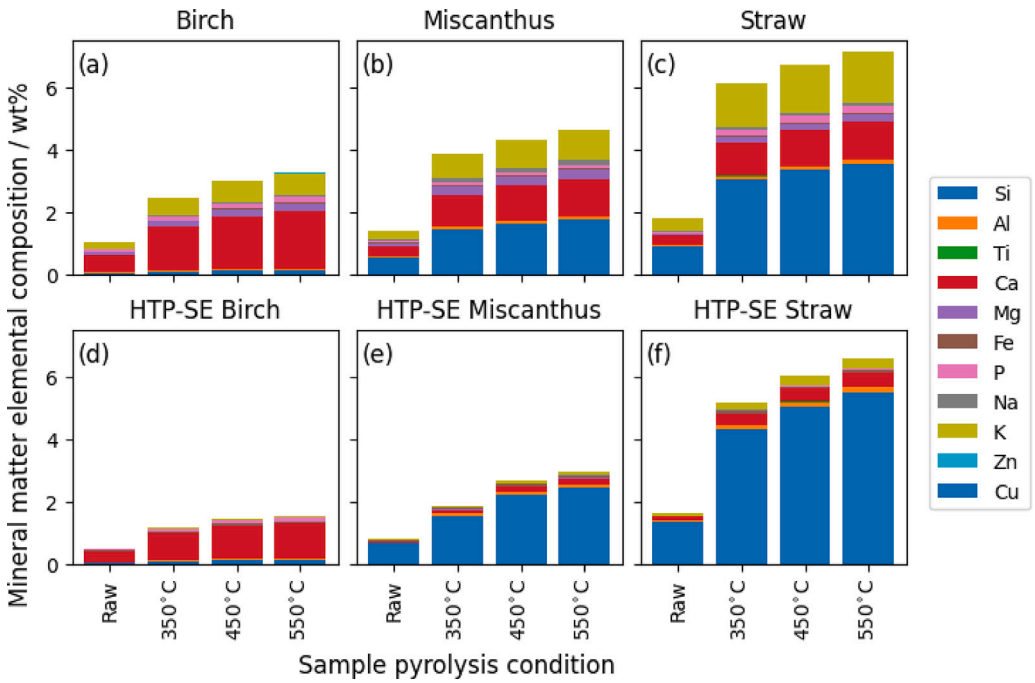

Fig. 5. Mineral matter elemental composition of biomass and produced biochars. (a) Birch (b) Miscanthus (c) Straw (d) HTP-SE Birch (e) HTP-SE Miscanthus (f) HTP-SE Straw.

birch showed the highest RRs. Again, this resulted from the respective changes in these materials' hemicellulose, ash, and oxygen content. The highest RR was achieved in the HTP-SE birch at 550 °C. This produced a value of 0.87, which is greater than the RR of many of the coals utilised in blast furnace coal injection blends. All the HTP-SE materials produced biochars from 350 °C with RRs that could be considered within an injection blend, as do the untreated miscanthus biochars. The untreated birch biochars produced at 450 °C and 550 °C could also be considered within an injection blend. The untreated straw biochars would be less likely to be considered for injection based upon the generated RRs. HTP-SE allows for biochars with greater RRs to be produced under lower temperature pyrolysis conditions. This could allow for lower operating costs and greater biochar yields.

HTP-SE may reduce the variability of HHV and RR, although further study would be required to verify this. Considering the importance of thermal and reactivity stability for efficient blast furnace operation, this would be beneficial. Any potential reduction in variability arising from HTP-SE could serve to homogenise biomass from different sources and seasons.

3.2.3. The effect of HTP-SE on biochar ash composition

The ash composition of solid fuels is an important consideration for any user, whether in the power industry, the steel industry, or elsewhere. Operators of biomass boiler systems experience a range of ash-related problems, including issues with alkali metals and chlorides (Abioye et al., 2024). Coal ash composition affects many process parameters in the steel industry. In the blast furnace, coal ash basicity, alkali, and phosphorus content all influence the process. The replacement of coal with biochar will likely affect these parameters. Whilst no adverse effects on EAF slag chemistry or steel quality were detected from biochar usage in the GREENEAF project, likely due to significantly lower coal/biochar usage rates than in a blast furnace, high potassium and chlorine levels could lead to corrosion in off-gas systems (Bianco et al., 2013).

Biomass contains essential inorganic elements like K, P, Fe, and Ca (Abioye et al., 2024). The HTP-SE process reduced the quantities of elements such as calcium, magnesium, phosphorus, sodium, potassium, and zinc, while conserving or concentrating iron and silicon, as shown in Fig. 5. This reduction in elemental content decreased the B3 basicity of material ashes (birch decreased from 7.91 to 4.67; miscanthus reduced from 0.55 to 0.05; and straw decreased from 0.26 to 0.05). Adjustments to blast furnace burden chemistry may be necessary to maintain slag basicity. The extent of element removal by HTP-SE depends on the acid used in pretreatment, with stronger acids potentially reducing the value of co-product liquors (Walker et al., 2018; Shrotri et al., 2017).

The alkali load (K_2O + Na_2O) is an important parameter in blast furnace operation. Alkalis have several negative influences on blast furnace operation: they catalyse the reverse Boudouard reaction, increasing the fuel rate; they promote the degradation of coke and ferrous material, which can lead to poorer permeability and affect productivity; they can lead to the formation of scaffolds and scabs, which can affect furnace stability and pose a safety risk; and lastly, they attack refractory linings, reducing the campaign length of a furnace (Geerdes et al., 2020).

The alkalis enter the blast furnace via the ferrous burden and carbonaceous material. Due to the blast furnace's varying temperature range, the alkalis take part in a cycle of reduction, oxidation, vaporisation, and condensation. Whilst a portion of the alkalis are removed in the slag and through the top gas, recirculation of 3 to 10 times the alkali input has been measured (Geerdes et al., 2020). Small increases in the alkali input can substantially affect overall blast furnace alkali levels.

Fig. 6a shows the calculated alkali loading of a blast furnace when replacing the coal injection with 175 kg/t_{HM} of biomass or biochar. 175 kg/t_{HM} is a representative injection rate of many blast furnaces worldwide and was also the average historical coal injection rate at Port Talbot prior to the degeneration of on-site assets (Geerdes et al., 2020; Babich et al., 2008). This would be a reasonable estimation of the volume of material that could be supplied through the injection system without additional investment and in the case of the 550 °C biochars, especially, would not require a large change to the coke rate due to the favourable RR. The mean total alkali load in Port Talbot blast furnaces over the studied period was 2.40 kg/t_{HM} with a standard deviation of 0.65 kg/t_{HM}. The alkali loading from the coke and burden accounted for around 2.07 kg/t_{HM}. This was added to the alkali loading from the injection of 175 kg/t_{HM} of biomass or biochar to calculate the total

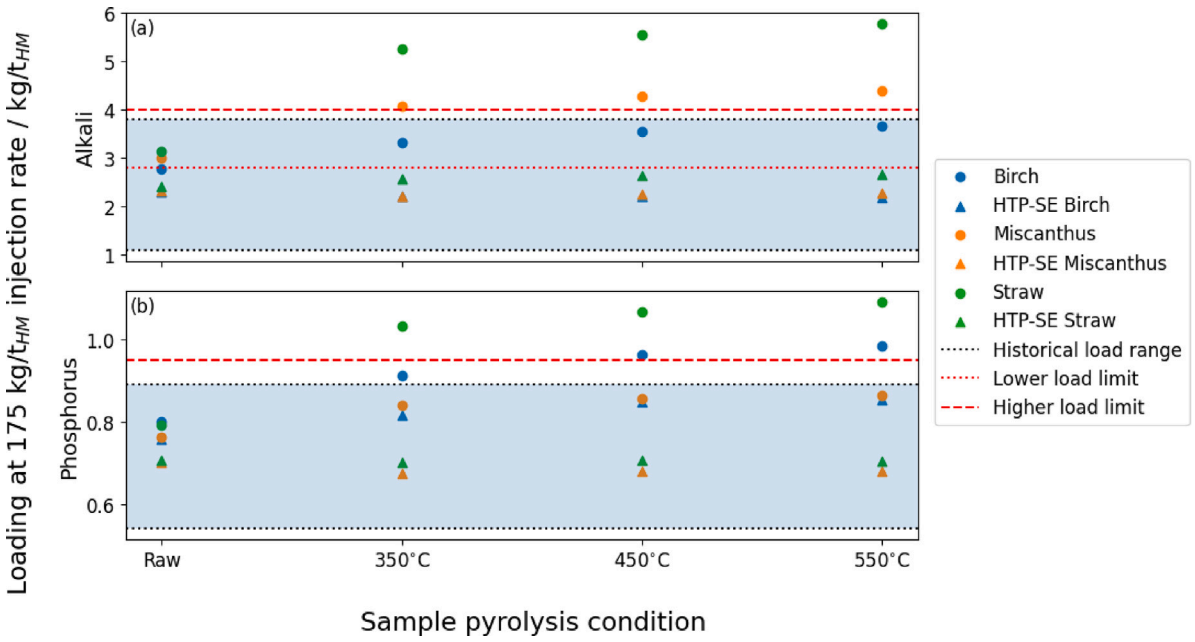

Fig. 6. Blast furnace (a) alkali (K_2O + Na_2O) loading and (b) phosphorus loading when replacing coal injection with biomass/biochar injection at an injection rate of 175 kg/t_{HM}.

alkali load, with adjustments made for additional coke requirements. The lower alkali load limit was 2.8 kg/t_{HM}, whilst the higher alkali load limit was 4.0 kg/t_{HM}. The lower limit was utilised under normal operating conditions whilst the higher limit was used when there were financial incentives to do so, such as utilising large volumes of reverts or raw materials with a high cost benefit. Globally, alkali inputs commonly range between 1.5 to 5 kg/t_{HM} (Geerdes et al., 2020; Babich et al., 2008).

Herbaceous biomass, such as straw and miscanthus, usually contain greater proportions of alkalis than woody biomass (Wolbers et al., 2018). In the case of the utilisation of untreated straw biochar, this would increase the alkali loading of the blast furnace to unacceptable levels. When using untreated miscanthus biochar, the alkali load is also undesirable and extends above the higher alkali load limit. The alkali load resulting from the untreated birch biochars would exceed the lower alkali load limit but would remain within historical operating levels. The effect of HTP-SE on the alkali load is apparent. All of the HTP-SE feedstock produced a calculated alkali loading well within usual operating conditions and under the lower alkali limit. In the case of the HTP-SE birch and miscanthus, the alkali load was reduced to less than the mean historical value of 2.40 kg/t_{HM}. This is highly beneficial and shows that HTP-SE can effectively mitigate one of the major problems of using biomass materials within the blast furnace.

Fig. 6b shows the calculated phosphorus loading of a blast furnace when replacing the coal injection with 175 kg/t_{HM} of biomass or biochar. Port Talbot's phosphorus limit on the blast furnace hot metal was 0.095%. As 90%–100% of phosphorus leaves the blast furnace via the hot metal; this level was controlled by controlling the amount of phosphorus entering the furnace in the raw materials (Babich et al., 2008). This equates to a load limit of 0.95 kg/t_{HM}, which is representative of a typical blast furnace operation (Geerdes et al., 2020). During the analysed historical period, furnace phosphorus load ranged from 0.54 kg/t_{HM} to 0.89 kg/t_{HM}. For reference, coal injection contributed an average of 0.06 kg/t_{HM} during this time.

When injecting raw biomass, all samples' calculated phosphorus load was well within the historical operating range. As the biochar pyrolysis temperature was increased and mineral matter was concentrated, phosphorus loading increased. In the case of the untreated birch and straw, this rose the phosphorus load above the load limit, making these materials unsuitable when replacing all of the injection coal. The untreated miscanthus contained less phosphorus than the other raw materials; as such, the calculated phosphorus loading remained within the historical load range. However, as the pyrolysis temperature increased, the phosphorus load approached the upper end of the historical load range and towards the load limit. This would remove any headroom to accommodate the use of high phosphorous reverts or sinter in the blast furnace, which could influence profitability.

HTP-SE had a beneficial effect on biochar phosphorus, (Fig. 6). In the birch sample, HTP-SE reduced phosphorus by 38%, bringing the phosphorus load below the load limit and within the historical load range. The reduction in phosphorus was greater in the miscanthus and straw samples, with HTP-SE reducing phosphorus levels by 89% and 90%, respectively. This reduced the phosphorus loading to below the historical mean of 0.72 kg/t_{HM}. This is beneficial and shows that HTP-SE can effectively mitigate the high phosphorus levels in biomaterials.

3.3. Investigating the cause of reduced HTP-SE biochar reactivity

The reduced reactivity of HTP-SE biochars will likely benefit their application to the steel industry. Char gasification reactivity has been shown to correlate strongly with char burnout, which could have implications for injection practices in blast furnace or electric arc furnace applications (Steer et al., 2018; Bianco et al., 2013; Cirilli et al., 2018). The cause of the reduced reactivity has been investigated by SEM imaging, analysis of the reaction kinetics, and by FTIR analysis.

3.3.1. SEM imaging of biochars

SEM images of the 550 °C biochars of birch, miscanthus, straw and their HTP-SE counterparts were taken, (see Supplementary Material Figure S1). In general, there were not many significant indicators of physical structural change that could explain the reduced reactivity of HTP-SE biochar, for example a reduction in pores or a decrease in surface area; however, there were still some notable changes occurring as a result of HTP-SE. There was evidence of plastic deformation in the HTP-SE birch biochar possibly due to lignin softening and repolymerisation (Dong et al., 2024). There was also the liberation of calcium carbonate particles following HTP-SE which were initially fixed within plant structures, therefore displaying that HTP-SE is a physical destructive process. The principle observation in the miscanthus biochar was

the cleavage of the biomass to yield a more fibrous HTP-SE residue. The straw biochar did not show obvious changes in particle shape and size following HTP-SE; however, there was the liberation of silica mineral structures as a result of HTP-SE.

3.3.2. TGA kinetics

The activation energies of the test materials undergoing CO_2 gasification were calculated from volumetric, grain, and random pore models using the methodology described by Alsawadi et al. (2025). These can be seen in Table S5 (see Supplementary Material). Activation energy is closely linked to the rate of a reaction. Therefore, biochars with higher activation energies can be expected to display larger $t_{0.5}$ values, as discussed in Section 3.2.The HTP-SE biochar samples exhibited increased activation energies in all cases compared to the untreated biochars. The increased activation energies of the HTP-SE biochars could be explained by the removal of catalytic compounds, such as calcium or potassium (as shown in Section 3.2.3), by the HTP-SE process, or by the increased stability of the carbon macromolecule. This suggests a chemical change was the cause of the reduced reactivity, which is further interrogated in Section 3.3.3. For steelmaking applications, the increase in activation energy and reduction in reactivity makes HTP-SE biochar a more suitable candidate for replacing fossil fuel carbon than conventional biochar. Materials with similar reactivities to coal and fossil carbon offer greater potential as drop-in replacements.

3.3.3. FTIR of biochars

FTIR spectra of biochars (see Supplementary Material Figures S2 and S3) produced at 550 °C were produced and the relative differences in spectra between the biochars produced from the untreated material and the HTP-SE counterpart were examined. See Supplementary Material Table S6 for the origin, group wavenumber, and the assignment of relevant FTIR peaks. Each biochar showed peaks between 700 and 850 cm^{-1}. The biochars were made 550 °C and have lost between 70%–80% of their original mass. It is therefore likely that much of the remaining material in the char is lignin or a lignin derivative as much of the hemicellulose and cellulose would have thermally decomposed (Zhao et al., 2014; Shen and Gu, 2009). Lignin is an aromatic molecule, therefore, it is possible that these peaks were caused by the aromatic C–H out-of-plane bend. The aromatic in-plane bend peaks overlap significantly with many C–O and C–O–C peaks in the 1000–1300 cm^{-1} range and are therefore not easily distinguished. The peaks around 1600 cm^{-1} can likely be attributed to aromatic ring stretching, whilst the small peaks around 1700 cm^{-1} correspond to C=O bonds. A clear set of peaks corresponding to carbonates existed in all untreated samples, whilst these were reduced in the HTP-SE samples, which corresponds with the findings in Section 3.2.3.

The relative differences in spectra between the biochars produced from the untreated material and the HTP-SE counterpart displayed the compositional changes caused by HTP-SE. The data up to 800 cm^{-1} was noisy and due to the mean offsetting of the spectra, may not have represented an actual change (see Supplementary Material Figure S3. The negative peaks at 874 cm^{-1} and 1420 cm^{-1} corresponded to carbonates reduction. The cause of the reductions around 1000 cm^{-1} in the miscanthus and straw samples were hard to identify due to the overlapping of peaks in this region; however, as there was a significant increase in absorbance around 1610 cm^{-1}, which would likely correspond to an increase in aromatic ring structures, the negative peak around 1000 cm^{-1} was more likely to have been caused by a reduction in C–O bonds in molecules such as primary alcohols, which would be more readily cleaved from the material's molecular structure during the HTP-SE process. An increase in C–O–C bonds in the ethers that join lignin monomers may explain the broad peak between 1100–1300 cm^{-1}. The final peak around 1720 cm^{-1} corresponded to an increase in C=O bonds, which may be generated by ketones or esters linking aromatic compounds.

Increasing the aromaticity of the material, creating more cross-linkages between molecules, and increasing the quantity of double bonds will all contribute to reducing the overall reactivity of the biochar and likely explains the reduced CO_2 gasification reactivities of the HTP-SE biochars discussed in Section 3.2.

3.4. Investigating biochar use on blast furnace parameters using a heat and mass balance model

Table S7 (see Supplementary Material) displays the dry coke rate requirement of a blast furnace, modelled using a Heat and Mass Balance Model under all coke operation, with 175 kg/t_{HM} coal injection, and with 175 kg/t_{HM} biochar injection. The model was set to maintain a top gas temperature of 120 °C with oxygen enrichment calculated accordingly. The offset fossil fuel CO_2 has been calculated by considering the average carbon contents of the fossil fuels and the related mass loss of converting coking coal to coke. Emissions relating to the energy used in the production of the materials or in ancillary processes have not been considered and would likely reduce these savings.

Biochar injection had a clear effect on the dry coke rate, with increases required from the coal injection scenario for all biochars. The largest increase was for the straw biochar, which was expected because it had the lowest RR, as discussed in Section 3.2.2. This would likely make this scenario financially nonviable. HTP-SE decreased the required coke rate for both the birch and straw, whilst there was a small increase for the miscanthus. This was due to the use of data discussed in Section 3.2.2, where the HHV and RR of the miscanthus and HTP-SE miscanthus 550 °C biochars had closely overlapping error ranges. Therefore, the related offset fossil fuel CO_2 is greatest in the HTP-SE birch biochar injection scenario. With current EU Emissions Trading System CO_2 allowances trading at around €80, this would result in a monetary value of over €135,000,000/yr for a plant producing 3,000,000 t_{HM}/yr. Whether these savings would offset the price of the additional coke usage would depend on the cost of raw materials. Additional financial arguments can be made if the biochar is produced on-site as this would allow for the use of generated syngas, whilst the sale of the hemicellulose liquor extracted during the HTP-SE process would also provide significant financial benefit.

In the model, operating conditions are calculated to accommodate biochar injection while maintaining furnace stability, which among other things, is indicated by top gas temperature. The top gas temperature is strongly related to the flame temperature. Flame temperature is affected by blast oxygen enrichment, blast volume, blast temperature, moisture, injectant volume, and injectant proximate and ultimate analysis (Geerdes et al., 2020). The biochars in this study had a greater requirement for hot blast and oxygen than the reference coal. This could negatively affect the economics of replacing coal with biochar, where increased blast energy and oxygen are used for maintaining stable operating conditions under biochar injection rather than providing reductions to the coke rate. Under normal conditions, an increase in blast temperature or volume increases the flame temperature by introducing more heat to the furnace. This can lead to a reduction in coke rate and an increase in productivity (Singh et al., 2018). On the other hand, following a coal-biomass co-injection trial, it was observed that coal utilisation improved alongside a reduction in flame temperature due to increased dispersion of all fuel particles in the raceway (Dang et al., 2024). Therefore, it is possible that partial replacement of coal with biochar could enhance furnace performance.

3.5. The effect of HTP-SE on the value of syngas produced during biomass pyrolysis

Table S8 (see Supplementary Material) shows the final compositions of dry accumulated syngases during the pyrolysis of the test materials at 550 °C. The effect of HTP-SE on the produced syngas is most readily

seen in the lower and higher heating values and in the relative compositions of H_2, CH_4, and C_2H_6. The syngases produced from the HTP-SE materials have higher energy densities than those produced from the untreated materials. The greatest increase in energy density can be seen in the straw samples, where the energy density of the produced syngas is increased by 39%. The relative changes in composition caused the increases in syngas energy densities. HTP-SE reduces the proportion of H_2 in each syngas, increasing both CH_4 and C_2H_6. The HHV of H_2 is 12.1 MJ/m^3; in comparison, the HHVs of CH_4 and C_2H_6 are 37.7 and 66.4 MJ/m^3, respectively. The increase in syngas hydrocarbons can likely be attributed to carbon concentration and oxygen reduction in the HTP-SE materials, as discussed in Section 3.1. The HTP-SE had no clear effect on the relative levels of CO and CO_2 in the syngas.

The increased energy density of the syngas is beneficial for many steelmaking applications. In the blast furnace stoves, where gas flow volumes have a maximum limit and, in Port Talbot, operated with an average mixed gas lower heating value (LHV) of 4.2 MJ/m^3, an increased LHV of an enriching gas, such as natural gas or coke oven gas, allows for greater use of low-energy gases, such as blast furnace top gas, reducing the need for flaring and increasing process efficiency. In an electric arc furnace application, an increase in energy density would reduce the required flow of gas that is needed to offset natural gas combustion. This may reduce the cost of engineering work required to adapt the process from natural gas use. Other potential avenues for biosyngas utilisation within the steel industry include combustion within an on-site power plant, conversion to biomethane, or use within a DRI plant. In each of these instances, a greater degree of methanation in the syngas, as resulting from HTP-SE, is advantageous.

3.6. The effect of HTP-SE on condensate production

The water-free mass yields and maximum HHVs of condensates produced in the 550 °C pyrolysis conditions used in the gas analysis experiment were calculated. These can be seen in Table S9 (see Supplementary Material). Water-free mass yield and maximum energy content were calculated by difference and using the assumption that chemical energy was conserved throughout the pyrolysis, which introduces error. These calculations suggest that condensate was the predominant pyrolysis product for most of the sample materials under these conditions. HTP-SE resulted in an increase in calculated water-free condensate yield for all materials and an increase in energy content for the birch and miscanthus. This was coupled with a decrease in syngas yield from all the HTP-SE materials. This is likely a result of the increased aromaticity and thermal stability of HTP-SE materials, as shown in Section 3.3.3. The calculated HHV values correspond with those found in literature and represent an energy source that could be further utilised, either by direct combustion or through a cracking process to produce energy-dense syngases (Sukiran et al., 2021; Ling et al., 2015). Alternatively, selling collected bio-oil for refining or use in carbon sequestration may be financially attractive. Direct measurement of condensate yield, HHV, and composition should be explored in future studies to confirm these suggestions and to establish the best use.

4. Conclusions

This study highlights the benefits of Hydrothermal Pretreatment-Steam Explosion (HTP-SE) of biomass for the steel industry and the potential to work synergistically with a hemicellulose extraction process for application in biobased products. HTP-SE enhances biochar quality by increasing carbon and hydrogen content, improving the Higher Heating Value (HHV) and Replacement Ratio (RR), making it comparable to coal. HTP-SE removes mineral matter, reducing ash, alkali metals, and phosphorus, which are crucial for Blast Furnace applications, and lowers biochar reactivity, potentially beneficial for Electric Arc Furnace applications. HTP-SE minimises Blast Furnace biochar injection's negative impacts, reduces coke rate and flame temperature, and increases offset fossil fuel CO_2. Additionally, it enhances produced syngas energy density by increasing methane and ethane content. These improvements suggest the potential for full replacement of injection coal in steelmaking, though further investigation is needed.

CRediT authorship contribution statement

Chay A. Davies-Smith: Writing – review & editing, Writing – original draft, Visualization, Validation, Software, Project administration, Methodology, Investigation, Formal analysis, Conceptualization. **Julian Herbert:** Writing – review & editing, Writing – original draft, Validation, Project administration, Methodology, Investigation, Formal analysis, Conceptualization. **Ciarán Martin:** Writing – review & editing, Supervision, Project administration, Funding acquisition, Conceptualization. **Darbaz Khasraw:** Project administration, Methodology, Investigation, Formal analysis, Conceptualization. **David Warren-Walker:** Writing – review & editing, Resources, Methodology, Investigation. **David Bryant:** Writing – review & editing, Investigation, Funding acquisition, Conceptualization. **Joe Gallagher:** Writing – review & editing, Investigation, Funding acquisition, Conceptualization. **Gordon Allison:** Resources, Methodology, Formal analysis. **Julian M. Steer:** Writing – review & editing, Resources. **Richard Marsh:** Writing – review & editing, Resources. **Ahmed Alsawadi:** Methodology, Formal analysis. **Rakesh Bhatia:** Writing – review & editing, Investigation, Funding acquisition, Conceptualization.

Declaration of competing interest

The authors declare that they have no known competing financial interests or personal relationships that could have appeared to influence the work reported in this paper.

Acknowledgements

This work was produced through the collaboration of projects from several funders, to whom the authors wish to give thanks. This work was funded by the Biotechnology and Biological Sciences Research Council Institute Strategic Programme Grants (BBS/E/IB/230001C, BB/P017460/1, and BB/S011994/1), Biotechnology and Biological Sciences Research Council MAXFEED follow-on fund (APP35058), Llywodraeth Cymru Welsh Government Project (2023/SFIS Level 1/031), and Tata Steel UK Ltd. The authors would like to thank Kelly Jenkins and the rest of the team at Tata Steel UK's BOS Laboratory for their help with the analysis of biomass ash. The authors would also like to thank Zhiming Yan and Bharath Sampath Kumar of Warwick University for their assistance in the analysis of pyrolysis syngas.

Appendix A. Supplementary data

Tables, SEM images, and FTIR spectra can be found in the Supplementary Material available with the online version of this paper.

Supplementary material related to this article can be found online at https://doi.org/10.1016/j.biortech.2025.133009.

Data availability

Data has been made available at DOI:10.17632/ypbr4mb24w.3.

References

Abatzoglou, N., Chornet, E., Belkacemi, K., Overend, R.P., 1992. Phenomenological kinetics of complex systems: the development of a generalized severity parameter and its application to lignocellulosics fractionation. Chem. Eng. Sci. 47, 1109–1122. http://dx.doi.org/10.1016/0009-2509(92)80235-5.

Abioye, K.J., Harun, N.Y., Sufian, S., Yusuf, M., Jagaba, A.H., Ekeoma, B.C., Kamyab, H., Sikiru, S., Waqas, S., Ibrahim, H., 2024. A review of biomass ash related problems: Mechanism, solution, and outlook. J. Energy Inst. 112, 101490. http://dx.doi.org/10.1016/j.joei.2023.101490.

Ahmad, E., Pant, K.K., 2018. Lignin conversion: A key to the concept of lignocellulosic biomass-based integrated biorefinery. Waste Biorefinery 409–444. http://dx.doi.org/10.1016/B978-0-444-63992-9.00014-8.

Alsawadi, A.M., Marsh, R., Steer, J.M., Morgan, D., 2025. A study of the mechanisms associated with CO2 utilisation via the reverse boudouard reaction. Fuel 381, 133448. http://dx.doi.org/10.1016/j.fuel.2024.133448.

Amado-Fierro, Á., Centeno, T.A., Diez, M.A., 2023. Exploring hydrochars from lignocellulosic wastes as secondary carbon fuels for sustainable steel production. Materials 16, 6563. http://dx.doi.org/10.3390/ma16196563.

Babich, A., Senk, D., Gudenau, H.W., Mavrommatis, K.T., 2008. Ironmaking: Textbook. Mainz, Aachen.

Bhatia, R., Lad, J.B., Bosch, M., Bryant, D.N., Leak, D., Hallett, J.P., Franco, T.T., Gallagher, J.A., 2021. Production of oligosaccharides and biofuels from miscanthus using combinatorial steam explosion and ionic liquid pretreatment. Bioresour. Technol. 323, 124625. http://dx.doi.org/10.1016/j.biortech.2020.124625.

Bianco, L., Baracchini, G., Cirilli, F., Moriconi, A., Moriconi, E., Marcos, M., Demus, T., Echterhof, T., Pfeifer, H., Beiler, C., Griessacher, T., 2013. Sustainable EAF steel production (GREENEAF). European Commission, http://dx.doi.org/10.2777/44502.

Bin, Y., Hongzhang, C., 2010. Effect of the ash on enzymatic hydrolysis of steam-exploded rice straw. Bioresour. Technol. 101, 9114–9119. http://dx.doi.org/10.1016/j.biortech.2010.07.033.

Cardarelli, A., Barbanera, M., 2023. Substitution of fossil coal with hydrochar from agricultural waste in the electric arc furnace steel industry: A comprehensive life cycle analysis. Energies 16, 5686. http://dx.doi.org/10.3390/en16155686.

Cirilli, F., Mirabile, D., Bianco, L., Baraccini, G., Rekersdrees, T., Marcos, M., Sommerauer, T., Griessacher, T., Echterhof, T., Reichel, T., 2018. Biochar for a Sustainable EAF Steel Production (GREENEAF2) : Final Report. European Commission.

Cui, L., Liu, Z., Si, C., Hui, L., Kang, N., Zhao, T., 2012. Influence of steam explosion pretreatment on the composition and structure of wheat straw. BioResources 7, 4202–4213. http://dx.doi.org/10.15376/biores.7.3.4202-4213.

Custom Market Insights, 2024. Global xylitol market 2025–2034. URL https://www.custommarketinsights.com/report/xylitol-market/.

Dang, H., Xu, R., Zhang, J., Wang, M., Shi, J., Zhang, J., He, X., Jia, G., Hu, Z., Zhao, D., 2024. Theoretical and experimental investigation on the effect of biomass injection on the utilization factor of pulverized coal and the raceway state in blast furnace. Fuel 375, 132550. http://dx.doi.org/10.1016/j.fuel.2024.132550.

Davies-Smith, C.A., Steer, J.M., Marsh, R., Morgan, D., 2022. A study of the volatilisation of coal sulphur during combustion under conditions similar to a blast furnace raceway. Fuel 330, http://dx.doi.org/10.1016/j.fuel.2022.125552.

Department for Energy Security & Net Zero, 2023. Biomass strategy.

Dong, Z., Yang, H., Laine, R., Leclerc, S., Chen, L., Hua, D., Chen, H., 2024. A comprehensive in-situ analysis of lignin softening and pyrolysis mechanism. Proc. Combust. Inst. 40, 105603. http://dx.doi.org/10.1016/j.proci.2024.105603.

Feliciano-Bruzual, C., 2014. Charcoal injection in blast furnaces (Bio-PCI): CO2 reduction potential and economic prospects. J. Mater. Res. Technol. 3, 233–243. http://dx.doi.org/10.1016/j.jmrt.2014.06.001.

Future Market Insights Inc, 2023. Xylooligosaccharide market outlook (2023 to 2033). URL https://www.futuremarketinsights.com/reports/xylooligosaccharide-market.

Geerdes, M., Chaigneau, R., Lingiardi, O., Molenaar, R., van Opbergen, R., Sha, Y., Warren, P., 2020. Modern Blast Furnace Ironmaking: An Introduction, fourth ed. IOS Press BV, Amsterdam.

Hutton, G., Rhodes, C., Ward, M., Bolton, P., 2023. UK Steel Industry: Statistics and Policy. House of Commons Library.

Kim, D., Park, K.Y., Yoshikawa, K., 2017. Conversion of municipal solid wastes into biochar through hydrothermal carbonization. Eng. Appl. Biochar. http://dx.doi.org/10.5772/intechopen.68221.

Li, X., Jia, H., Jiang, L., Mou, Z., Zhang, B., Zhang, Z., Chen, Y., 2024. Biochar prepared from steam-exploded bitter melon vine for the adsorption of methylene blue from aqueous solution: Kinetics, isotherm, thermodynamics and mechanism. Sustainability 16, 7278. http://dx.doi.org/10.3390/su16177278.

Ling, C.K., San, H.P., Kyin, E.H., Hua, L.S., Chen, L.W., Yee, C.Y., 2015. Yield and calorific value of bio oil pyrolysed from oil palm biomass and its relation with solid residence time and process temperature. Asian J. Sci. Res. 8, 351–358. http://dx.doi.org/10.3923/ajsr.2015.351.358.

Markets and Markets, 2023. Furfural market. URL https://www.marketsandmarkets.com/Market-Reports/furfural-market-101056456.html.

Mathieson, J.G., Rogers, H.P., Somerville, M., Ridgeway, P., Jahanshahi, S., 2011. Use of biomass in the iron and steel industry - an Australian perspective.

Mishra, R.K., kumar, V., Kumar, P., Mohanty, K., 2022. Hydrothermal liquefaction of biomass for bio-crude production: A review on feedstocks, chemical compositions, operating parameters, reaction kinetics, techno-economic study, and life cycle assessment. Fuel 316, 123377. http://dx.doi.org/10.1016/j.fuel.2022.123377.

Overend, R.P., Chornet, E., 1987. Fractionation of lignocellulosics by steam-aqueous pretreatments. Philos. Trans. R. Soc. Lond. Ser. A Math. Phys. Sci. 321, 523–536. http://dx.doi.org/10.1098/rsta.1987.0029.

Pedersen, M., Meyer, A.S., 2010. Lignocellulose pretreatment severity - relating pH to biomatrix opening. New Biotechnol. 27, 739–750. http://dx.doi.org/10.1016/j.nbt.2010.05.003.

Qian, C., Li, Q., Zhang, Z., Wang, X., Hu, J., Cao, W., 2020. Prediction of higher heating values of biochar from proximate and ultimate analysis. Fuel 265, http://dx.doi.org/10.1016/j.fuel.2019.116925.

Sarker, T.R., Ethen, D.Z., Nanda, S., 2024. Decarbonization of metallurgy and steelmaking industries using biochar: A review. Chem. Eng. Technol. 47, http://dx.doi.org/10.1002/ceat.202400217.

Sexton, D.C., Steer, J.M., Marsh, R., Greenslade, M., 2018. Investigating char agglomeration in blast furnace coal injection. Fuel Process. Technol. 178, 24–34. http://dx.doi.org/10.1016/j.fuproc.2018.05.013.

Shen, D., Gu, S., 2009. The mechanism for thermal decomposition of cellulose and its main products. Bioresour. Technol. 100, 6496–6504. http://dx.doi.org/10.1016/j.biortech.2009.06.095.

Shrotri, A., Kobayashi, H., Fukuoka, A., 2017. Catalytic conversion of structural carbohydrates and lignin to chemicals. Adv. Catal. 60, 59–123. http://dx.doi.org/10.1016/bs.acat.2017.09.002.

Singh, R.K., Sudhir, S., Kumar, R.R., Jha, V.K., Das, B.K., Mallick, A., Pan, S.K., Arora, A., 2018. Increasing BF hot blast temperature. Steel Times Int. 42, 33–34, 36–37.

Sluiter, J., Sluiter, A., Scarlata, C., Templeton, D., Crocker, D., Hames, B., 2012. Determination of structural carbohydrates and lignin in biomass: Laboratory analytical procedure (LAP) (revised august 2012): Issue date: 4/25/2008. Supercedes July 2011 version.

Sluiter, J., Sluiter, A., Scarlata, C., Templeton, D., Hames, B., 2008. Determination of sugars, byproducts, and degradation products in liquid fraction process samples: Laboratory analytical procedure (LAP).

Steer, J.M., Marsh, R., Sexton, D., Greenslade, M., 2018. A comparison of partially burnt coal chars and the implications of their properties on the blast furnace process. Fuel Process. Technol. 176, 230–239. http://dx.doi.org/10.1016/j.fuproc.2018.03.027.

Strauss, W., Schmidt, L., 2018. Are black pellets ready to compete with white pellets?. https://biomassmagazine.com/articles/are-black-pellets-ready-to-compete-with-white-pellets-15072. (Accessed 11 June 2024).

Suchsland, O., Lansing, E., Woodson, G.E., 1987. Fiberboard Manufacturing Practices Intlie United States. U.S. Department of Agriculture.

Sukiran, M.A., Loh, S.K., Bakar, N.A., 2021. Production of bio-oil from fast pyrolysis of oil palm biomass using fluidised bed reactor. Carbon Resour. Convers. 4, 239–250.

Walker, D.J., Gallagher, J., Winters, A., Somani, A., Ravella, S.R., Bryant, D.N., 2018. Process optimization of steam explosion parameters on multiple lignocellulosic biomass using Taguchi method-a critical appraisal. Front. Energy Res. 6, http://dx.doi.org/10.3389/fenrg.2018.00046.

Wang, M., Jia, T., Wang, J., Hu, Y., Liu, F., Wang, H., Chang, L., 2016. Changes of sulfur forms in coal after tetrachloroethylene extraction and theirs transformations during pyrolysis. Fuel 186, 726–733. http://dx.doi.org/10.1016/j.fuel.2016.09.007.

Wang, M., Liu, L., Wang, J., Chang, L., Wang, H., Hu, Y., 2015. Sulfur K-edge XANES study of sulfur transformation during pyrolysis of four coals with different ranks. Fuel Process. Technol. 131, 262–269. http://dx.doi.org/10.1016/j.fuproc.2014.10.038.

Wang, F., Ouyang, D., Zhou, Z., Page, S.J., Liu, D., Zhao, X., 2021. Lignocellulosic biomass as sustainable feedstock and materials for power generation and energy storage. J. Energy Chem. 57, 247–280. http://dx.doi.org/10.1016/j.jechem.2020.08.060.

Wei, R., Zheng, X., Zhu, Y., Feng, S., Long, H., Xu, C.C., 2024. Hydrothermal bio-char as a foaming agent for electric arc furnace steelmaking: Performance and mechanism. Appl. Energy 353, 122084. http://dx.doi.org/10.1016/j.apenergy.2023.122084.

Wolbers, P., Cremers, M., Robinson, T., Madrali, S., Tourigny, G., 2018. Biomass Pre-Treatment for Bioenergy. IEA Bioenergy.

worldsteel, 2022. World steel in figures 2022. https://worldsteel.org/data/world-steel-in-figures-2022/. (Accessed 11 June 2024).

Yu, Y., Wu, J., Ren, X., Lau, A., Rezaei, H., Takada, M., Bi, X., Sokhansanj, S., 2022. Steam explosion of lignocellulosic biomass for multiple advanced bioenergy processes: A review. Renew. Sustain. Energy Rev. 154, 111871. http://dx.doi.org/10.1016/j.rser.2021.111871.

Zhao, J., Xiuwen, W., Hu, J., Liu, Q., Shen, D., Xiao, R., 2014. Thermal degradation of softwood lignin and hardwood lignin by TG-FTIR and Py-GC/MS. Polym. Degrad. Stab. 108, 133–138. http://dx.doi.org/10.1016/j.polymdegradstab.2014.06.006.

Ziegler-Devin, I., Chrusciel, L., Brosse, N., 2021. Steam explosion pretreatment of lignocellulosic biomass: A mini-review of theorical and experimental approaches. Front. Chem. 9, http://dx.doi.org/10.3389/fchem.2021.705358.

Zoghlami, A., Paës, G., 2019. Lignocellulosic biomass: Understanding recalcitrance and predicting hydrolysis. Front. Chem. 7, http://dx.doi.org/10.3389/fchem.2019.00874.